5. CONCLUSION

In this study, actively and passively excited sinusoidal two types of antenna, which are PCB strip and microstrip antenna are investigated at the operating frequencies of K and millimeter wave bands. Passively excited sinusoidal antenna is applied to PCB strip and microstrip structures for the first time. It is aimed to create more rigid and smaller-sized sinusoidal antennas than the wire type. It is shown that the sinusoidal PCB strip antennas can be formulated by the same manner of wire type of antennas. The measured patterns of investigated PCB strip antennas are compared also with calculated patterns obtained from a written MATLAB code. The measured patterns of actively excited antennas are compared with the simulated ones obtained from HFSS program as well. The reduction in the size of antenna dimensions are achieved 50% for microstrips and 20% for PCB strip antennas. Phase velocity calculated for PCB strip structures are 15% smaller than wire structures. This reduction in the phase velocities of PCB strip antennas is high because the thickness of PCB strip is large (approximately 1 λ). The advantage of passive excitation, an array can be composed by repeating a number of sinusoidal parts. The electromagnetic energy is coupled to sinusoidal parts by a long Goubau line in this case.

REFERENCES

1. W. Rothman and N. Karas, The sandwich wire antenna: A new type of microwave line source radiator, IRE Int Convention Record 5 (1957), 166–172.
2. W. Rothman and N. Karas, Printed circuit radiators: The sandwich wire antenna, Microwave J 2(1959), 29–33.
3. V.G. Trentini, Flachantenne mit periodisch gebogenem Leiter, Frequenz 14 (1960), 239–243.
4. K. Chen, Sandwich-wire antenna, IRE Trans Antenna Prop 10 (1962), 159–164.
5. H.E. Green and J.L. Whitrow, A new analysis of the sandwich-wire antenna, IEEE Trans Antenna Prop 19 (1971), 600–605.
6. A.O. Salman, D. Dibekci, S. Gavrilov, and A.A. Vertiy, The millimeter-wave radiation of a traveling-wave sinusoidal wire antenna, IEEE Trans Antenna Prop, editing.
7. G. Goubau, Surface waves and their application to transmission lines, J Appl Phys 21 (1950), 1119–1128.
8. A.O. Salman, D. Dibekci, S. Gavrilov, and A.A. Vertiy, The millimeter-wave radiation properties of a novel wire antenna for the security fence radar, IEEE Trans Antenna Prop, editing.
9. A.A. Vertiy, S.P. Gavrilov, I.V. Voynovskyy, and S. Ozbek, Security perimeter fence for littoral protection, Proceedings of New Concepts for Harbour Protection, Littoral Security and Shallow-Water Acoustic Communication, 3–8 June, Istanbul, Turkey, 2005, pp. 199–208.
10. J.R. James, P.S. Hall, and C. Wood, Microstrip antenna theory and design, Peter Peregnus, London, 1986, pp. 125–127.
11. L. Safai, A.A. Sebak, Radiation characteristics of microstrip serpent antennas, Antenna Prop Soc Int Symp 22 (1984), 55–57.
12. C. Wood, Curved microstrip lines as compact wide band circularly polarized antennas, Microwaves Opt Acoust 3(1979), 5–13.

A SINGULARITY EXTRACTION TECHNIQUE FOR COMPUTATION OF ANTENNA APERTURE FIELDS FROM SINGULAR PLANE WAVE SPECTRA

Cecilia Cappellin,[1,2] Olav Breinbjerg,[1] and Aksel Frandsen[2]
[1]Ørsted·DTU, Technical University of Denmark, DK-2800 Kgs. Lyngby, Denmark
[2]TICRA, Læderstræde 34, DK-1201 Copenhagen K, Denmark; Corresponding author: cc@ticra.com

Received 2 October 2007

ABSTRACT: *An effective technique for extracting the singularity of plane wave spectra in the computation of antenna aperture fields is proposed. The singular spectrum is first factorized into a product of a finite function and a singular function. The finite function is inverse Fourier transformed numerically using the Inverse Fast Fourier Transform, while the singular function is inverse Fourier transformed analytically, using the Weyl-identity, and the two resulting spatial functions are then convolved to produce the antenna aperture field. This article formulates the theory of the singularity extraction technique and illustrates the effect of this for an array of electric Hertzian dipoles.* © 2008 Wiley Periodicals, Inc. Microwave Opt Technol Lett 50: 1308–1312, 2008; Published online in Wiley InterScience (www.interscience.wiley.com). DOI 10.1002/mop.23346

Key words: *plane wave expansion, singularity extraction; fast Fourier transform, Weyl-identity*

1. INTRODUCTION

The plane wave expansion (PWE) is widely used in antenna theory, as well as diffraction, imaging, and propagation theory, to represent the electromagnetic field in source-free regions of space as an infinite, continuous spectrum of plane waves [1–3]. The plane wave spectrum (PWS) of the PWE is an analytic function on the entire spectral domain, except possibly at the circular border between the visible and invisible spectral regions where a singularity may exist [4]. Since the PWS at, and close to, this circular border corresponds to the far-field radiation pattern at wide angles, a zero of the pattern at those angles is a necessary condition for the PWS to be finite. Otherwise, the PWS possesses a singularity there, and this is thus the case for most antennas.

In applications where the aperture field is calculated from the PWS this singularity must be taken properly into account to ensure the accuracy of the aperture field. In some cases, e.g., where the PWS is determined from a planar near-field measurement over a finite scan plan, the PWS is reliable only over the central part of the visible region of the spectral domain [5], and the part of the domain where the singularity exists must be disregarded. However, in other cases, e.g., where the PWS is determined from a far-field measurement, a compact range measurement or a spherical near-field measurement, the PWS at, or close to, the border between the visible and invisible regions can be determined and the singularity is thus known.

Since the PWS and the aperture field constitute an inverse Fourier transform pair, the Inverse Fast Fourier Transform (IFFT) is normally used for computation of the aperture field from the PWS. However, the singularity of the PWS, though integrable, prevents a straightforward application of the IFFT. Many singularity extraction techniques for numerical integration have been proposed, in particular for integral equation and method of moment techniques [6, 7], but here a different approach is used.

The purpose of this work is to formulate and validate a new singularity extraction technique for the computation of antenna

aperture fields from singular plane wave spectra. In this technique the singular PWS is first factorized into a product of a finite function and a singular function. The inverse Fourier transforms of these two spectral functions are then calculated. For the finite function this is done numerically using the IFFT, and for the singular function this is done analytically using the Weyl-identity. Finally, the two thus obtained spatial functions are convolved to produce the antenna aperture field. In this work the effect of the singularity extraction technique is applied to a simple test case to isolate and identify the singularity and its influence on the aperture field. However, the singularity extraction technique has been applied also to real measurements data for practical and complicated antennas [8, 9]. The present manuscript is organized as follows: in Section 2 the PWE theory is briefly summarized with particular attention to the singularity. In Section 3 the singularity extraction technique is formulated, while Section 4 illustrates its effect through a numerical test case. All expressions are given in the S.I. rationalized system with a suppressed $e^{-i\omega t}$ time convention.

2. THE PLANE WAVE EXPANSION

The PWE of the electric field $\bar{E}$, valid for $z > z_o$ with z_o being the largest z-coordinate of the antenna as indicated in Figure 1(a), is given by [4]

$$\bar{E}(x,y,z) = \frac{1}{2\pi}\int_{-\infty}^{\infty}\int_{-\infty}^{\infty} \bar{T}(k_x,k_y)e^{ik_z z}e^{i(k_x x+k_y y)}dk_x dk_y$$

$$= F^{-1}\{\bar{T}(k_x,k_y,z)\},\ z > z_o \quad (1a)$$

where (x,y,z) are the Cartesian coordinates of the observation point with position vector $\bar{r}$, while k_x and k_y are the spectral variables which together with $k_z = \sqrt{k^2 - k_x^2 - k_y^2}$, with k being the wavenumber, constitute the Cartesian components of the wave propagation vector $\bar{k}$. Eq. (1a) shows that the two-dimensional inverse Fourier transform (IFT), F^{-1}, of the PWS for a given z-coordinate $z > z_o$, $\bar{T}(k_x,k_y,z) \equiv \bar{T}(k_x,k_y)e^{ik_z z}$, provides the electric field $\bar{E}$at that z-plane. The inverse of Eq. (1a) is obviously

$$\bar{T}(k_x,k_y,z) = \frac{1}{2\pi}\int_{-\infty}^{\infty}\int_{-\infty}^{\infty} E(x,y,z)e^{i(k_x x+k_y y)}dx\,dy = F\{\bar{E}(x,y,z)\},z$$

$$> z_o \quad (1b)$$

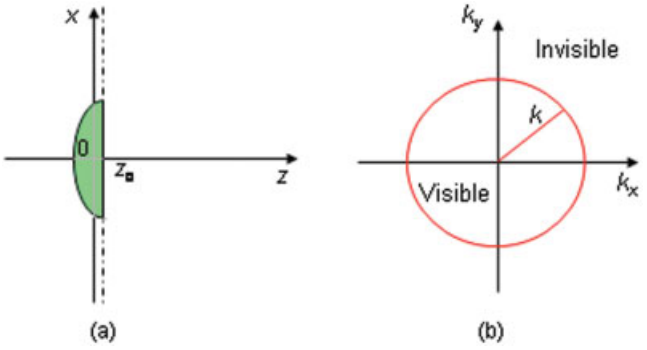

Figure 1 PWE for a general antenna: (a) Spatial domain of validity, $z > z_o$, (b) visible and invisible regions of the spectral $k_x k_y$-domain. [Color figure can be viewed in the online issue, which is available at www.interscience.wiley.com]

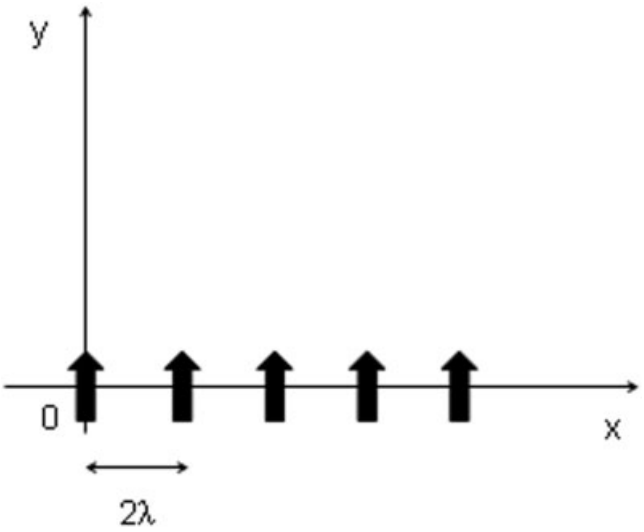

Figure 2 Array of five y-oriented electric Herzian dipoles displaced on the x-axis

The spectral $k_x k_y$-domain is divided into two regions, see Figure 1(b). The visible region, for $k_x^2 + k_y^2 \le k^2$, contains propagating plane waves and the invisible region, for $k_x^2 + k_y^2\ k^2$, contains evanescent plane waves. The two spectral variables k_x andk_y are real, while k_z is real in the visible region but purely imaginary with a positive imaginary part in the invisible region to satisfy the radiation condition. Since the evanescent plane waves are exponentially attenuated with increasing z-coordinate, their contribution to the field is usually negligible at distances larger than one wavelength from the antenna [3]. In practice, the k_x- and k_y-integrals are truncated at finite values $\pm k_{x\max}$ and $\pm k_{y\max}$, respectively, and in cases where the PWS is obtained from measurements, the PWS is reliable only over the visible region or an even smaller spectral domain [5].

The PWS is an analytic function on the entire spectral domain except possibly at the border between the visible and invisible region where $k_z = 0$ and a singularity of the type $1/k_z$ often exists in one or more of its components [4]. This constitutes the only possible singularity and a necessary but insufficient condition to prevent its existence is a null in the xy-plane of the antenna far-field pattern. While the singularity in the PWS does not explicitly appear in Eq. (1b), it is seen when $\bar{T}(k_x,k_y)$is expressed as a function of the volume current density $\bar{J}$of the antenna [4]

$$\bar{T}(k_x,k_y) = \frac{1}{k_z}\frac{1}{4\pi k\eta}\bar{k}\times\left(\bar{k}\times\int_V \bar{J}(\bar{r})e^{i(k_x x+k_y y+k_z z)}dV\right) \quad (2)$$

with η being the medium intrinsic admittance, or when the visible region of $\bar{T}(k_x,k_y)$is expressed in terms of the far-field pattern [4],

$$\bar{E}_{far}(r,\theta,\varphi) = \lim_{kr\to\infty}\bar{E}(r,\theta,\varphi) =$$

$$-\frac{e^{ikr}}{r}ik\cos\theta\bar{T}(k\sin\theta\cos\varphi, k\sin\theta\sin\varphi)\ \theta\in[0,\pi/2],\ \varphi\in[0,2\pi] \quad (3)$$

since $k\cos\theta = k_z$.

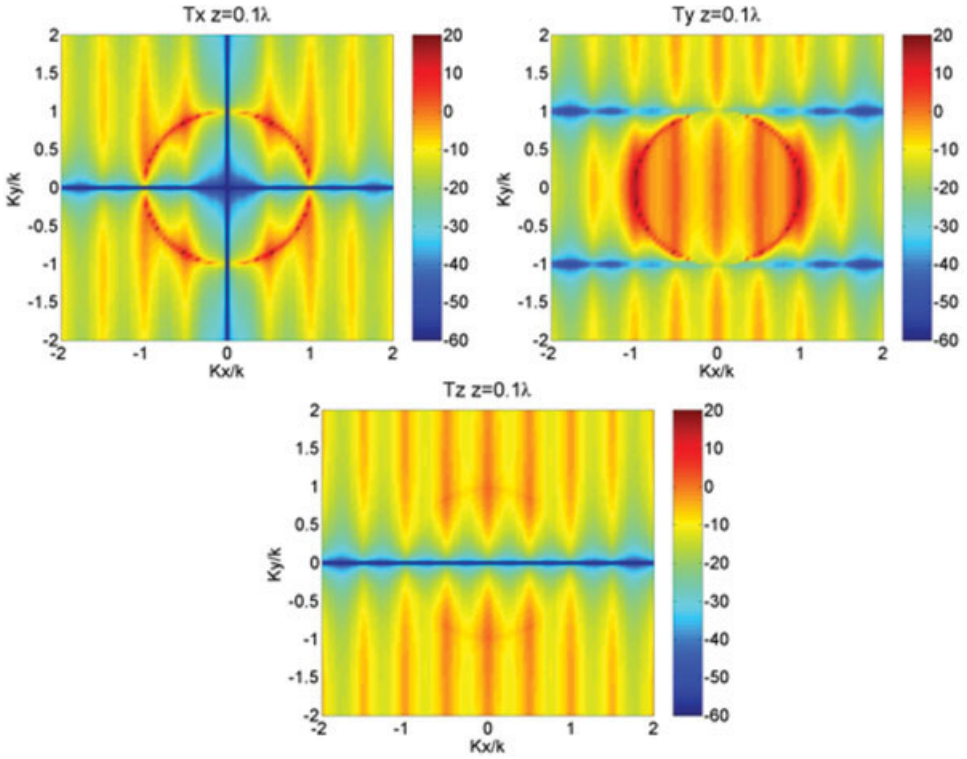

Figure 3 Amplitude of the Cartesian components of the PWS $\bar{T}$for the array of Hertzian dipoles in dB scale and normalized to the center value of T_y, on the $z = 0.1\lambda$ plane. [Color figure can be viewed in the online issue, which is available at www.interscience.wiley.com]

3. THE SINGULARITY EXTRACTION TECHNIQUE

Though the singularity of $\bar{T}(k_x,k_y)$is integrable, a direct use of the IFFT results in an inaccurate aperture field unless the singularity is sampled very densely. While on one hand this could in principle be possible, on the other hand such a high density would be necessary over the entire k_xk_y-domain to have the uniform sampling required by the IFFT algorithm. This presents a problem when the PWS is obtained from measurements since a very dense angular or spatial sampling, in θ- and φ-coordinates for far-field measurements or in x- and y-coordinates for planar near-field measurements, is then required. Another possible approach is to employ a special numerical integration scheme incorporating a singularity extraction technique like for example is shown in [6, 7]. Finally, it is possible to transform the Cartesian spectral variables into spherical spectral variables in which case the singularity disappears. However, in both cases one would loose the advantages of the IFFT.

Here, we propose to defactorize the spectrum $\bar{T}$into a product of two functions, the finite $\bar{T}_1$and the singular $1/k_z$ whereby

$$\bar{T}(k_x,k_y) = \bar{T}_1(k_x,k_y)\frac{1}{k_z}. \tag{4}$$

Since the IFT of a product of two spectral functions is equal to the convolution of the two corresponding spatial functions [10] the integral of Eq. (1a) is effectively solved since the IFT of the finite $\bar{T}_1$can be computed numerically by the IFFT and the IFT of the singular $1/k_z$ is computed analytically using the Weyl-identity [4]

$$\frac{e^{ikr}}{i2\pi r} = \frac{1}{2\pi}\int_{-\infty}^{\infty}\int_{-\infty}^{\infty}\frac{1}{k_z}e^{i(k_xx+k_yy+k_zz)}dk_xdk_y \quad z>0. \tag{5}$$

Thus Eq. (1a) is rewritten as follows,

$$\bar{E}(x,y,z) = \frac{1}{2\pi}\int_{-\infty}^{\infty}\int_{-\infty}^{\infty}\bar{T}(k_x,k_y)e^{ik_zz}e^{i(k_xx+k_yy)}dk_xdk_y \quad z>z_o$$

$$= \frac{1}{2\pi}\int_{-\infty}^{\infty}\int_{-\infty}^{\infty}\bar{T}_1(k_x,k_y)\frac{1}{k_z}e^{ik_zz}e^{i(k_xx+k_yy)}dk_xdk_y$$

$$= \frac{1}{2\pi}\int_{-\infty}^{\infty}\int_{-\infty}^{\infty}\bar{T}_1(k_x,k_y)e^{ik_z(z-z_1)}e^{i(k_xx+ky)}dk_xdk_y \otimes \frac{1}{2\pi}\int_{-\infty}^{\infty}\int_{-\infty}^{\infty}$$

$$\times\frac{1}{k_z}e^{ik_zz_1}e^{i(k_xx+k_yy)}dk_xdk_y = \bar{E}_1(x,y,z-z_1)\otimes\frac{e^{ikr_1}}{i2\pi r_1} \tag{6}$$

As it is seen in Eq. (6), the z-coordinate is split in two $z = (z - z_1) + z_1$ and hence $r_1 = \sqrt{x^2+y^2+z_1^2}$. This is done to have an exponential term of the type of e^{ik_zz}in both factors, to use the Weyl identity of Eq. (5) and ensure an accurate implementation of the convolution, as explained in the following.

From a computational point of view the following important observations can be made.

First it is noted that, in practical implementations of Eqs. (1a) and (6), the PWS is known only at $N \times N$ discrete points on a finite $\pm k_{x\max}$ and $\pm k_{y\max}$ domain and thus with sampling densities $\Delta k_x = 2k_{x\max}/(N-1)$and $\Delta k_y = 2k_{y\max}/(N-1)$, respectively.

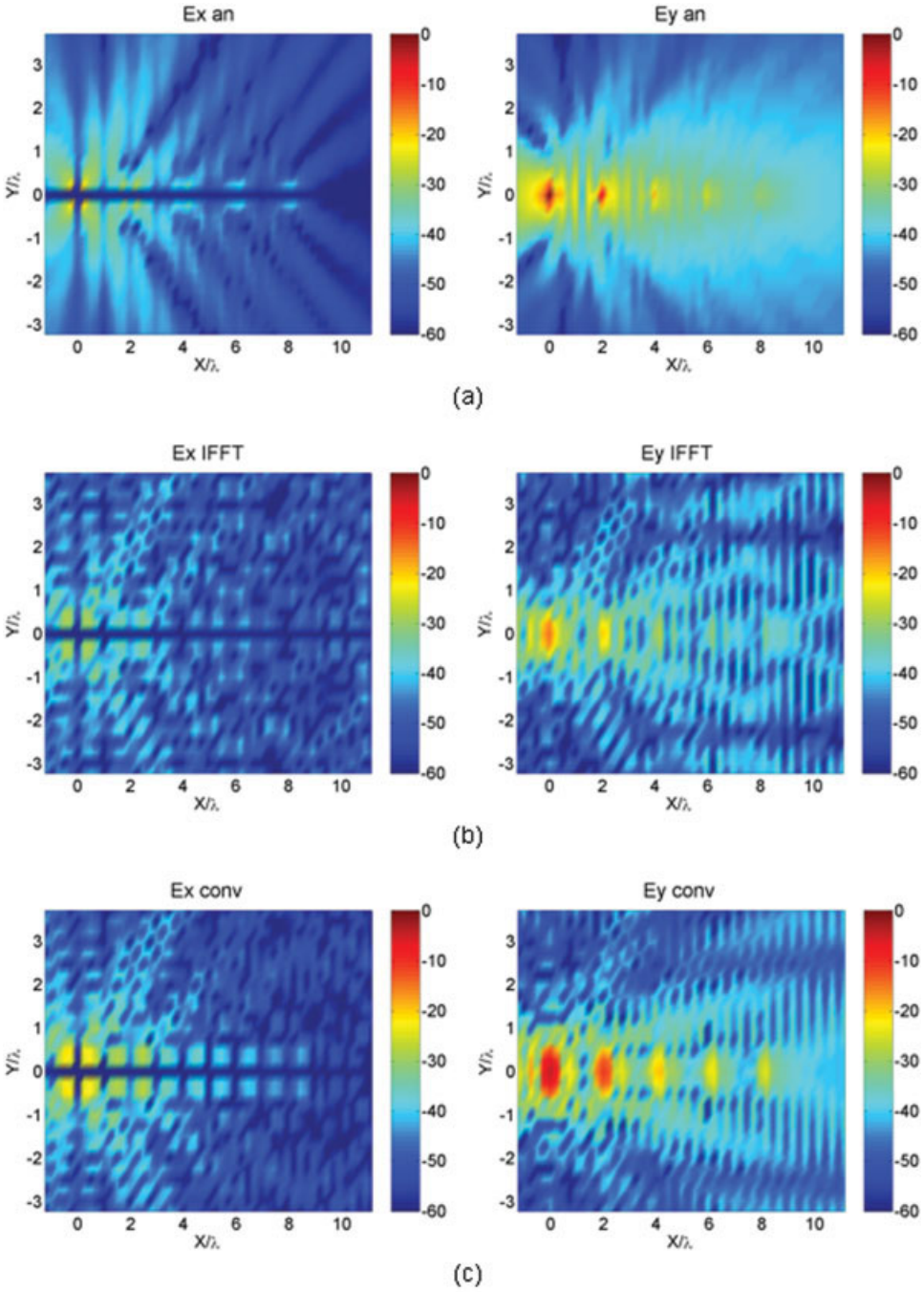

Figure 4 Amplitude of the x- and y-component of the electric field in dB scale at $z = 0.1\lambda$ normalized to the maximum of the y-component of the analytical field: (a) analytical field, (b) IFFT of the visible region of the PWS without the singularity extraction, (c) IFT of the visible region of the PWS with the singularity extraction. [Color figure can be viewed in the online issue, which is available at www.interscience.wiley.com]

In virtue of the Nyquist sampling criterion and the discrete Fourier transform theory, the transformed electric field is also given at $N \times N$ discrete points centered at the origin and with sampling densities $\Delta x = 2\pi/(\Delta k_x N)$and $\Delta y = 2\pi/(\Delta k_y N)$, respectively [3].

Second we notice that the Green's function, that is usually computed at the same $N \times N$ discrete spatial points (the Green's function can however be computed on an even larger xy-domain, provided that the sampling in x- and y- is maintained, since we know its expression analytically), is azimuthally symmetric and, once convolved with the function $\bar{E}_1$, it provides the electric field $\bar{E}$at $(2N - 1) \times (2N - 1)$ discrete points.

Third, though the result of Eq. (6) is in principle independent of the chosen z_1, the result is accurate only when the truncation errors of the two spatial functions on the chosen xy-domain are negligible. For the AUT considered in Section 4 which has a size of 8λ, a z-coordinate less than 0.2λ ensures $\bar{E}_1$values with negligible truncation error on the $[-30\lambda: 30\lambda]$ xy-domain and a z_1-plane of about 0.01λ provides the Green's function with a sufficient decay on the same spatial region. The effect of the convolution will always be that of a more accurate field; however, for small z_1-values the Green's function is very peaked and it may happen that the effect is qualitatively limited.

Fourth, if we want to compute the electric field $\bar{E}$only on a certain spatial window of the entire *xy*-domain, whether centered or not, we can easily modify the convolution algorithm by providing as input the function $\bar{E}_1$on the desired *xy*-window, as long as a sufficient decay of $\bar{E}_1$is ensured. The Green's function can also be considered on a window smaller than the entire *xy*-domain, provided that such a window is centered at the origin and a decay of at least 60 dB from the peak is ensured. By doing that, the computational time for the convolution drastically diminishes.

Fifth, it is noted that the singularity extraction technique provides the correct aperture field also for nonsingular spectral components and the technique can thus be applied to all components of the PWS without a priori considerations on the absence or presence of the singularity.

4. TEST CASE

To illustrate the effect of the singularity extraction technique presented in Section 3, we investigate here an array of 5 *y*-oriented electric Hertzian dipoles displaced along the *x*-axis at a distance of 2λ from each others, see Figure 2. The excitations of the five dipoles are *P*, *P*/2, *P*/5, *P*/8, and *P*/10, respectively, with *P* being the dipole moment of the dipole at the origin. The exact PWS is first computed from Eq. (2) on the $[-2k : 2k]$ $k_x k_y$-domain with 91 sampling points in both directions, see Figure 3. The PWS clearly shows the singularity in both the *x*- and *y*-components. In the computation of the aperture field from this PWS, only the visible region is taken into account since this is most often the case in practice, while the invisible region is zero-padded.

Figure 4a shows the analytical *x*- and *y*-components of the electric field on the $z = 0.1\lambda$ plane while Figure 4(b) shows the result of a straightforward IFFT of the singular PWS without the use of the singularity extraction technique. It is evident that while all five dipoles are seen in Figure 4(a), only the first two are clearly distinguished in Figure 4(b). The last three dipoles, having a weaker excitation, can not be correctly detected since the singularity is not properly taken into account. Figure 4(c) then shows the result of applying the singularity extraction technique. In this case all five dipoles are clearly detected and the difference in their excitations can also be seen. The slightly wider extensions of these compared to the analytical result is due to the truncation of the PWS to the visible region and the truncation of the two functions involved in the convolution on the finite *xy*-plane.

5. CONCLUSIONS

An effective technique to extract the singularity of plane wave spectra in the computation of antenna aperture fields has been presented. The algorithm is based on the Inverse Fast Fourier Transform and Weyl-identity and allows the accurate computation of the aperture field when a dense sampling in the spectral domain is not possible. The detection of sources of very weak amplitude has been verified by a numerical example and the evident advantages compared to the Inverse Fast Fourier Transform of the PWS without the singularity extraction have been underlined.

REFERENCES

1. A.J. Devaney, A filtered backpropagation algorithm for diffraction tomography, Ultrason Imag 4 (1982), 336–360.
2. T.B. Hansen and P.M. Johansen, Inversion scheme for ground penetrating radar that takes into account the planar air-soil interface, IEEE Trans Geosci Remote Sens 38(2000), 496–506.
3. J.J.H. Wang, An examination of the theory and practices of planar near/field measurement, IEEE Trans Antenna Propagat 36 (1988), 746–753.
4. T.B. Hansen and A.D. Yaghjian, Plane wave theory of time-domain fields, near-field scanning applications, IEEE Press, New York, NY, 1999.
5. A.D. Yaghjian, Upper-bound errors in far-field antenna parameters determined from planar near-field measurements, Part I: Analysis, Nat Bur Stand Tech Note 667, Boulder, CO, (1975).
6. A.D. Yaghjian, Electric dyadic Green's functions in the source region, Proc IEEE 68 (1980), 248–263.
7. M.G. Duffy, Quadrature over a pyramid or cube of integrands with a singularity at a vertex, SIAM J Numer Anal 19 (1982), 1260–1262.
8. C. Cappellin, A. Frandsen, and O. Breinbjerg, Application of the SWE-to-PWE antenna diagnostics technique to an offset reflector antenna, AMTA Antenna Measurements Technique Association Symposium, St. Louis, USA, November 2007.
9. C. Cappellin, A. Frandsen, S. Pivnenko, G. Lemanczyk, and O. Breinbjerg, Diagnostics of the SMOS radiometer antenna system at the DTU-ESA spherical near-field antenna test facility, EuCAP European Conference on Antennas and Propagation, Edinburgh, UK, November 2007.
10. A. Papoulis, Signal analysis, McGraw-Hill, 1977.

DESIGN AND ANALYSIS OF WIDEBAND DOUBLE-SIDED PRINTED SPIRAL-DIPOLE ANTENNA WITH CAPACITIVE COUPLING

Hatem Rmili[1] and Jean-Marie Floc'h[2]
1 ISSAT, Sidi Messaoud, 5111 Mahdia, Tunisie; Corresponding author: hatem.rmili@yahoo.fr
[2] IETR, UMR CNRS 6164, INSA, 20 avenue Buttes des Coësmes 35043 Rennes, France

Received 8 October 2007

ABSTRACT: *A compact and wideband printed dipole antenna is presented for C- and X-applications. The proposed balun-fed antenna consists of a double-sided printed dipole structure with a microstrip-fed modified spiral-dipole printed on the top side of the substrate, and a capacitive-coupling rectangular-patch, a connecting strip line and the ground plane printed on the bottom side. For the proposed antenna, a wide resonant band which extends from 6.27 to 12.47 GHz, with a fractional bandwidth of 66%, is observed. Details of the experimental and simulation results are presented and discussed.* © 2008 Wiley Periodicals, Inc. Microwave Opt Technol Lett 50: 1312–1317, 2008; Published online in Wiley InterScience (www.interscience.wiley.com). DOI 10.1002/mop.23341

Key words: *printed spiral; dipole antennas; wideband; capacitive coupling*

1. INTRODUCTION

Microstrip or patch antennas are widely used for microwave applications in a market driven by device miniaturization, as they are small and easily fabricated. In addition to their well-known advantages (low profile, low cost of fabrication, easy integration into planar arrays, light weight, and compatibility with microwave integrated-circuit technologies), broadening frequency bandwidth and sharing multifrequency bands are also desirables properties, especially with the rapid progress in wireless communication.

In particular, communication systems that operate in the C and X-bands are normally designed using separate antennas for each band. Since it is becoming more and more important to use such systems in one setting, it is desirable to design a single antenna that operates in both frequency bands [1]. To comply with this require-